British Journal of Pharmacology (2004) 142, 899–911
www.nature.com/bjp

Neuroprotective efficacy and therapeutic time window of peroxynitrite decomposition catalysts in focal cerebral ischemia in rats#

[1]Meenakshisundaram Thiyagarajan, [1]Chaman Lal Kaul & *,[1]Shyam Sundar Sharma

[1]Department of Pharmacology and Toxicology, National Institute of Pharmaceutical Education and Research (NIPER), Sector-67, S.A.S. Nagar, Mohali, Punjab, India

1 Free radicals have been implicated in cerebral ischemia reperfusion (IR) injury. Massive production of nitric oxide and superoxide results in continuous formation of peroxynitrite even several hours after IR insult. This can produce DNA strand nicks, hydroxylation and/or nitration of cytosolic components of neuron, leading to neuronal death. Peroxynitrite decomposition catalysts 5,10,15,20-tetrakis(*N*-methyl-4′-pyridyl)porphyrinato iron (III) (FeTMPyP) and 5,10,15,20-tetrakis(4-sulfonatophenyl)porphyrinato iron (III) (FeTPPS) have been demonstrated to protect neurons in *in vitro* cultures; however, their neuroprotective efficacy in cerebral IR injury has not been explored.

2 In the present study, we investigated the efficacy and the therapeutic time window of FeTMPyP and FeTPPS in focal cerebral ischemia (FCI).

3 FCI was induced according to the middle cerebral artery occlusion (MCAO) method. After 2 h of MCAO and 70 h of reperfusion, the extent of neurological deficits, infarct and edema volume were measured in Sprague–Dawley rats.

4 FeTMPyP and FeTPPS were administered at different time points 2, 6, 9 and 12 h post MCAO. FeTMPyP and FeTPPS (3 mg kg^{-1}, i.v.) treatment at 2 and 6 h post MCAO produced significant reduction in infarct volume, edema volume and neurological deficits. However, treatment at latter time points did not produce significant neuroprotection.

5 Significant reduction of peroxynitrite in blood and nitrotyrosine in brain sections was observed on FeTMPyP and FeTPPS treatment.

6 As delayed treatment of FeTMPyP and FeTPPS produced neuroprotection, we tested whether treatment had any influence over the apoptotic neuronal death. DNA fragmentation and *in situ* nick end-labeling assays showed that FeTMPyP and FeTPPS treatment reduced IR injury-induced DNA fragmentation.

7 In conclusion, peroxynitrite decomposition catalysts (FeTMPyP and FeTPPS) produced prominent neuroprotection even if administered 6 h post MCAO and the neuroprotective effect is at least in part due to the reduction of peroxynitrite and apoptosis.
British Journal of Pharmacology (2004) **142,** 899–911. doi:10.1038/sj.bjp.0705811

Keywords: Stroke; FeTMPyP; FeTPPS; focal ischemia; middle cerebral artery occlusion; oxidative stress; peroxynitrite; apoptosis; TUNEL

Abbreviations: ANOVA, one-way analysis of variance; FCI, focal cerebral ischemia; FeTMPyP, 5,10,15, 20-tetrakis(*N*-methyl-4′-pyridyl)porphyrinato iron (III); FeTPPS, 5,10,15,20-tetrakis(4-sulfonatophenyl)porphyrinato iron (III); FITC, fluorescein isothiocyanate; IR, ischemia reperfusion; MCAO, middle cerebral artery occlusion; NOS, nitric oxide synthase; PDC, peroxynitrite decomposition catalyst; ROS, reactive oxygen species; SOD, superoxide dismutase; TBS, Tris buffered saline; TUNEL, terminal deoxynucleotidyl transferase-mediated dUTP nick end labeling

Introduction

Stroke is the third cause of death after heart disease and cancer and is the leading cause of chronic disability in the developed countries. It occurs as a result of loss of blood supply or inadequate blood flow to a particular part of brain. The pathophysiological mechanisms leading to neuronal injury in ischemic stroke are complex and multifactorial. Involvement of oxidative stress in ischemic reperfusion (IR) injury is well established (Cuzzocrea *et al*., 2001). The contribution of components of reactive oxygen species (ROS) such as superoxide radical, hydroxyl radical, hydrogen peroxide, nitric oxide and peroxynitrite in producing neuronal loss after IR injury is considered to be substantial (Imaizumi *et al*., 1984; Kumura *et al*., 1996; Cuzzocrea *et al*., 2001). Superoxide can react with nitric oxide to form peroxynitrite and is found to be one of the highly toxic components of ROS. It can easily permeate lipid bi-layers (~400 times more permeable through lipid membrane as compared to superoxide) with a calculated permeability coefficient of $\sim 8 \times 10^{-4}$ cm s^{-1} (Marla *et al*., 1997), leading to peroxidation of membrane lipids (Radi *et al*.,

*Author for correspondence; E-mail: sssharma@niper.ac.in, shyamsharma14@yahoo.com
#NIPER Communication Number – 285
Advance online publication: 14 June 2004

1991). It can hydroxylate and nitrate aromatic residues of proteins and nucleotides (Beckman *et al*., 1992; Murakami *et al*., 1998). Peroxynitrite-mediated nitration of tyrosine residue inhibits the tyrosine phosphorylation and hence affects the signal transduction pathways like nerve growth factor signaling (Jonnala & Buccafusco, 2001). Peroxynitrite can also produce single- and/or double-strand breaks in DNA (King *et al*., 1992; Salgo *et al*., 1995). It can inactivate many cytosolic enzymes including aconitase (Castro *et al*., 1994) and superoxide dismutase (Smith *et al*., 1992; Beckman *et al*., 1994). It can form an adduct with carbon dioxide which is more toxic as compared to peroxynitrite itself (Denicola *et al*., 1996).

Several antioxidants (tempol, LY231617, LY178002 and melatonin) showed neuroprotection in cerebral IR injury and associated conditions (Clemens *et al*., 1991; Fuson *et al*., 1999; Cuzzocrea *et al*., 2000a; Gupta *et al*., 2004). The metalloporphyrin class of decomposition catalyst antioxidants are found to be highly potent because the concentration needed for activity is minimal as compared to other groups of compounds (Cuzzocrea *et al*., 2001). Many of them are reported to mimic superoxide dismutase (SOD) activity and decompose various components of ROS depending on the metallic ion present in the co-ordination complex (Patel & Day, 1999). Neuroprotective effects of the metalloporphyrin class of SOD mimetics such as MnTE-2-PyP(5+), AEOL 10113, AEOL 10150, M40403 and M40404 have been demonstrated in animal model of ischemia (Salvemini *et al*., 1999; Mackensen *et al*., 2001; Sheng *et al*., 2002). Peroxynitrite decomposition catalysts (PDCs) such as 5,10,15,20-tetrakis(*N*-methyl-4′-pyridyl)porphyrinato iron (III) (FeTMPyP) and 5,10,15,20-tetrakis(4-sulfonatophenyl)porphyrinato iron (III) (FeTPPS) (Figure 1) have been shown to protect cytokine-induced cytotoxicity in hippocampal culture (Misko *et al*., 1998) and methamphetamine-induced neurotoxicity in rats (Imam *et al*., 1999; 2001). PDCs are more potent than other groups of compounds which reduce $NO^{\bullet -}$ and $O_2^{\bullet -}$ formation and hence the peroxynitrite or direct peroxynitrite scavengers. PDCs isomerize peroxynitrite to nitrate anion and thereby decrease its decomposition to highly reactive intermediates such as nitrogen dioxide and hydroxyl radicals (Misko *et al*., 1998). In addition to the peroxynitrite decomposition effect, these compounds do have moderate superoxide dismutase activity. Though the neuroprotective effect of metalloporphyrin SOD mimetics has been demonstrated in cerebral ischemia models, the neuroprotective effect of PDCs has not been reported.

In the present study, we investigated the neuroprotective potential of PDCs (FeTMPyP and FeTPPS) in middle cerebral artery occlusion (MCAO)-induced focal cerebral ischemia in rats. According to the Stroke Therapy Academic Industry Roundtable (1999) recommendations, we also investigated the therapeutic time window of PDCs in cerebral ischemia. In addition to this, the possible mechanism(s) of neuroprotective activity of PDCs were also investigated.

Methods

Materials

Dihydrorhodamine123, rhodamine123, anti-mouse IgG were purchased from Sigma Chemical Company, U.S.A. FeTMPyP, FeTPPS, anti-nitrotyrosine antibody and proteinase K were purchased from Calbiochem, U.S.A. The 3-0 nylon monofilament (Ethilon®, Johnson & Johnson, India) was purchased locally. All other chemicals were of analytical grade or reagent grade purchased from commercial suppliers.

Animal preparation and middle cerebral artery occlusion (MCAO)-induced focal cerebral ischemia

Male Sprague–Dawley rats, weighing 240–260 g were obtained from Central Animal Facility, National Institute of Pharmaceutical Education and Research (NIPER). Animals were housed in a room at a temperature of $22 \pm 1^{\circ}C$ and 12 h dark and light cycle. Standard rat chow pellets and water were allowed *ad libitum*. All the procedures performed in the study were approved by Institutional Animal Ethics Committee, NIPER.

Overnight fasted rats were administered atropine sulfate ($0.5\,mg\,kg^{-1}$, i.p.) and anesthesia was induced using 4% halothane in a mixture of 70% nitrous oxide and 30% oxygen. Anesthesia was maintained by administering 1% halothane using the anesthesia system (Harvard Apparatus Ltd, Kent, U.K.) through the Coax Breathing Device® (Harvard Apparatus Ltd, Kent, U.K.). Femoral artery was cannulated for blood pressure recording and arterial blood sampling. The oxygen concentration in the anesthetic gas mixture was fine adjusted to get pO_2, pCO_2 and pH values close to the physiological limits. Focal cerebral ischemia was induced according to the MCAO method as previously described (Thiyagarajan & Sharma, 2004). Briefly, the left common carotid artery was exposed through midline incision. The external and internal carotid arteries were separated from the adhering tissue. The external carotid artery was ligatured and dissected. A 3-0 nylon monofilament with its tip rounded by gentle rubbing over sandpaper and subsequently coated with poly-L-lysine was advanced up to 21 mm from the lumen of external carotid artery into the internal carotid artery to block the left middle cerebral artery. After occlusion was achieved, the monofilament was secured in place with a ligature. The incision was sutured. Occlusion was done for a period of 2 h. For reperfusion the rats were anesthetized and the sutured wound was opened and the filament pulled out completely. Rats not showing neurological deficits immediately after reperfusion (neurological score <3) were excluded from the study. After 2 h of MCAO and 70 h of reperfusion, rats were killed and the brains isolated for estimation of infarct and edema volume. In the sham-operated group, only the filament was introduced into the external carotid artery but not advanced.

Physiological parameters

Physiological parameters were continuously monitored during surgery. Rats were allowed to breathe spontaneously during surgery. If the respiratory rate decreased or suffocation observed, artificial respiration was provided through an endotracheal tube using a respiratory pump (Inspira®, Harvard Apparatus Ltd, Kent, U.K.) which is in connection with the anesthesia system. Rectal temperature was continuously maintained ($37.0 \pm 0.5^{\circ}C$) using a feedback-controlled homeothermic blanket system (Harvard Apparatus Ltd, Kent, U.K.) and a heating lamp on the surgery table. Blood pressure was continuously recorded in a computer using UIM100c hardware and Acq *Knowledge* v3.7.3 software system (Biopac

Systems Inc., U.S.A.). Biochemical parameters like blood gases (pO_2 and pCO_2), pH, glucose and bicarbonate were measured 10 min before MCAO, 30 min after MCAO and 10 min after reperfusion using pHOx® plus L system (Nova Biomedical Corporation, U.S.A.).

Treatment schedule

A total of 166 rats were used to study various parameters. For neurological deficit, infarct and edema volume estimation rats were randomly divided into different groups. PDCs (FeTMPyP and FeTPPS) were administered after 2, 6, 9 or 12 h post MCAO. They were administered at a dose of 1 and 3 mg kg^{-1} at all time points except at 2 h post MCAO time point at which they were administered at 0.3 and 1 mg kg^{-1}. For all the studies drug was administered intravenously (i.v.) through the jugular vein. Each group had 4–7 rats (see Table 1 for the exact number of rats used in each group). For mechanistic studies, PDCs were administered 30 min post MCAO (Figure 2). This treatment schedule was necessary to clearly see their effects on biochemical parameters in ischemic and reperfusion phase.

Calculation of infarct and edema volume

Coronal sections of brain, 2-mm thick, were cut and stained with 2% triphenyl tetrazolium chloride (TTC) solution in saline for 10 min at 37°C. After fixing in 10% formal saline overnight, they were scanned using a flat bed scanner (Hewlett-Peckard Scan Jet ADF). The area of infarction was measured in coronal brain sections by using 'Leica Qwin' image analysis software. Infarct areas of all sections were cumulated to get total infarct area which was multiplied by thickness of brain sections to get the volume of infarction. Edema correction of infarct volume was done using the equation, volume correction = (infarct volume × contralateral volume)/ipsilateral volume. The volumes of both the hemispheres were calculated separately, from which edema volume was calculated by subtracting the contralateral volume from ipsilateral volume.

Assessment of neurological deficit

Neurological deficits in the vehicle-treated group and FeTMPyP- and FeTPPS-treated groups were measured according to the method of Longa *et al*. (1989) at 24, 48 and 72 h after MCAO (Longa *et al*., 1989). Neurological findings were scored on a five-point scale. No neurological deficit = 0, failure to extend right paw fully = 1, circling to right = 2, falling to right = 3 did not walk spontaneously and had depressed levels of consciousness = 4. The neurological scores of each rat were summed up to get the cumulative neurological score which was compared using Kruskal–Wallis one-way ANOVA on ranks. Neurological deficit scores were represented as median cumulative scores ±95% confidence intervals.

Estimation of peroxynitrite

Four groups (sham-, vehicle-, FeTMPyP- and FeTPPS-treated) each containing 3–4 rats were used for estimation of peroxynitrite in blood using a fluorescent dye dihydrorhodamine123 which gets oxidized to rhodamine123 in a peroxynitrite-dependent manner (Szabo *et al*., 1995). Rats were injected with dihydrorhodamine123 through the jugular vein (2×10^{-6} M, 1 ml kg^{-1} in saline) 1 h after MCAO. Vehicle or FeTMPyP/FeTPPS (3 mg kg^{-1}) treatment was done 30 min post MCAO. Rats were anesthetized 1 h after reperfusion (i.e. 2 h after dihydrorhodamine123 injection) and the blood was collected by cardiac puncture. The fluorescence in the plasma was measured using the spectrofluorometer (Perkin-Elmer, Norwalk, CT, U.S.A.) at an excitation wavelength of 500 nm

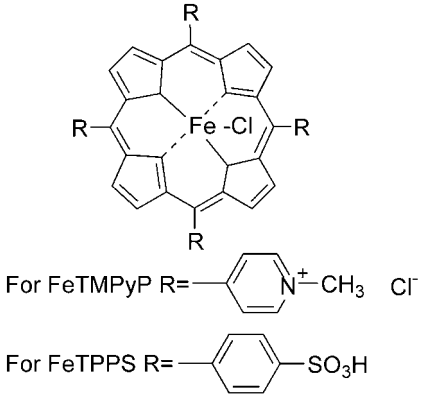

Figure 1 Chemical structure of PDCs 5,10,15,20-tetrakis (*N*-methyl-4′-pyridyl)porphyrinato iron (III) (FeTMPyP) and 5,10,15,20-tetrakis(4-sulfonatophenyl)porphyrinato iron (III) (FeTPPS).

Table 1 Infarct volume, edema volume and neurological score in FeTMPyP and FeTPPS-treated rats

Drug	*Vehicle*	*2* h, *0.3* mg kg^{-1}	*2* h, *1* mg kg^{-1}	*6* h, *1* mg kg^{-1}	*6* h, *3* mg kg^{-1}	*9* h, *1* mg kg^{-1}	*9* h, *3* mg kg^{-1}	*12* h, *1* mg kg^{-1}	*12* h, *3* mg kg^{-1}
FeTMPyP (n)	6	5	6	7	7	4	4	7	7
Infarct volume	203.0±12.6	103.2±15.4*	69.8±14.4*	138.9±13.4	125.6±10.2*	141.2±11.1	126.8±15.0	184.6±20.7	172.5±16.2
Edema volume	97.1±9.9	46.6±8.3	38.2±8.1*	65.3±12.7	53.9±7.1	73.9±6.7	65.8±14.6	72.1±14.7	64.7±11.7
Neurological score	9.5±2.0	7.0±4.1	4.0±2.5*	6.0±2.2	6.0±2.1	7.5±3.3	7.0±2.4	8.0±2.4	7.5±2.0
FeTPPS (n)	6	4	5	6	7	6	5	6	7
Infarct volume	203.0±12.6	116.5±5.7*	77.6±14.2*	146.7±18.1*	133.7±18.2*	156.8±9.2	153.2±7.8	163.1±114	169.1±21.7
Edema volume	97.1±9.9	47.0±1.9*	28.8±2.2*	55.5±24.1	48.0±10.7*	66.4±15.5	56.7±7.8	79.2±14.3	60.8±11.9
Neurological score	9.5±2.0	7.0±2.4	6.0±3.1	7.0±2.0	6.0±1.0	7.5±1.7	7.0±1.5	8.0±0.8	8.0±1.9

All the values are represented as mean±s.e.m., except neurological deficit which is represented as median±95% confidence interval. Neurological deficits were observed at 24, 48 and 72 h after MCAO. The median cumulative scores are presented here. FeTMPyP and FeTPPS treatment significantly decreased the infarct volume, edema volume and neurological score. Decrease in infarction was found to be prominent at striatum and cortex. *$P<0.05$ and **$P<0.01$ as compared to the vehicle-treated group.

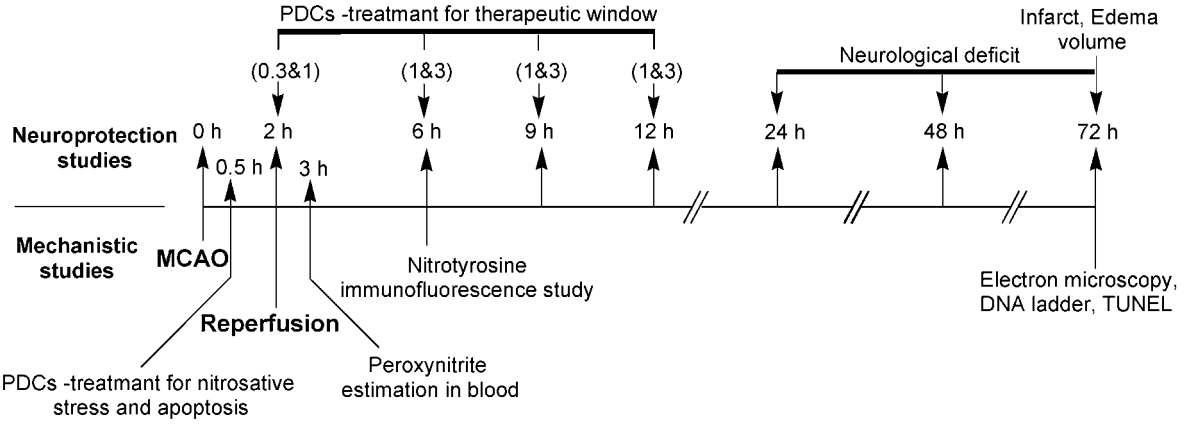

Figure 2 Study design for neuroprotective efficacy, therapeutic time window and mechanism of PDCs action: For neuroprotective efficacy and therapeutic time window, FeTMPyP and FeTPPS were tested at two dose levels (either 0.3 and 1 or 1 and 3 mg kg^{-1}) at 2, 6, 9, 12 h post MCAO along with a vehicle-treated control, which accounted for a total of 17 different groups of rats. The numbers mentioned in parenthesis are the doses (mg kg^{-1}). The times scheme, at which FeTMPyP and FeTPPS treatments were done after MCAO for different groups of animals, is indicated by their doses in parenthesis. Rats were killed 70 h post MCAO and extent of neurological damage was measured. For mechanistic studies PDCs were administered 30 min post MCAO. Peroxynitrite levels were estimated (dihydrorhodamine123 method) 3 h post MCAO and nitrotyrosine immunofluorescence analysis was performed 6 h post MCAO. DNA ladder, TUNEL and electron microscopy were conducted 72 h post MCAO.

and emission wavelength of 536 nm. The plasma level of rhodamine123 was calculated from the standard curve obtained from authentic rhodamine123 in a concentration of 0–10 nM prepared in plasma obtained from the untreated normal rats. Background plasma fluorescence was subtracted from all the samples.

Estimation of tyrosine nitration by immunofluorescence

Immunofluorescence of nitrotyrosine was performed to evaluate the increase in nitrosative stress presumably as a result of increased formation of peroxynitrite as described previously (Thiyagarajan & Sharma, 2004). Briefly four groups (sham-, vehicle-, FeTMPyP- and FeTPPS-treated) each containing three rats were anesthetized using chloral hydrate (400 mg kg^{-1}, i.p.) after 2 h of MCAO and 4 h of reperfusion. They were transcardially perfused with 200 ml of ice-cold phosphate-buffered saline followed by 500 ml of 4% buffered paraformaldehyde in saline (pH 7.4) for *in situ* fixation of brain. Brain was isolated and embedded in wax. Serial sections of 3 μm thickness were cut using microtome (Leica, Germany) and spread over microscopic slides. The sections at the level of anterior commissure, temporal limb (AP -0.26 to -0.51 mm to bregma) were selected from the series for immunofluorescence study. After hydration the sections were washed with TBS (Tris-buffered saline, 20 mM, pH 7.4), followed by incubation with 20 μg ml^{-1} of proteinase K for 20 min for antigen retrieval. Following a rinse with TBS, the sections were incubated with blocking buffer (5% goat serum in TBS) for 120 min. Endogenous biotin-binding sites were blocked by sequential incubation of avidin and biotin for 30 min each. The sections were then incubated with primary antibody mouse Anti-nitrotyrosine (Calbiochem, U.S.A.) in blocking buffer at 4°C overnight. The sections were washed three times with TBS and then incubated with biotin-conjugated anti-mouse IgG (Sigma-Aldrich Inc.) in blocking buffer for 2 h at 37°C. The specific labeling was detected using avidin-conjugated FITC system. The sections were observed under fluorescent microscope (Leica, Germany) and images were acquired with the CCD camera (DC300F, Leica). The images were analyzed using the image analysis software 'Leica Qwin' for the densitometry comparison. To observe the peroxynitrite decomposition effect of PDCs, vehicle or PDC treatment were done 30 min post MCAO.

Electron microscopy

Brain specimens from sham-operated and ischemic rats were examined for the features of apoptotic characteristics. 70 h after reperfusion, rats were anesthetized and transcardiac perfusion done as mentioned previously with 4% paraformaldehyde and 1% glutaraldehyde. Brain was isolated and 2-mm thick coronal sections were made. Brain tissues (1 mm^3 thick) were cut from the penumbral and necrotic area of third 2-mm coronal section. They were incubated in 4% paraformaldehyde and 1% glutaraldehyde overnight at 4°C followed by 0.5% osmium tetroxide. After dehydration, the samples were embedded in polyhydroxylated aromatic acrylic (LR white) embedding medium. Regions of interest were identified through light microscopy and the ultra thin sections were spread on the grids. After counter staining with uranyl acetate and lead citrate, they were visualized and photographed under electron microscope.

DNA fragmentation assay

DNA fragmentation is considered to be one of the important characteristic features of apoptotic cell death. Brain specimens from two groups (vehicle-, FeTMPyP-treated) each containing three rats, were used for DNA isolation. Rats were killed 70 h after reperfusion and brains isolated. Coronal sections of brain, 2-mm thick, were cut and stained with TTC as mentioned previously to identify the penumbral (borderline between the ischemic and normal tissue) area. The brain tissue from the third 2-mm ipsilateral cortex (penumbral zone) and ischemic cortex (necrotic zone) was used for DNA isolation.

Tissue samples were homogenized separately in digestion buffer (25 mM disodium EDTA, 100 mM sodium chloride, 10 mM Tris-HCl (pH 8) and 0.5% SDS). Samples were incubated overnight at 56°C after the addition of proteinase K to a final concentration of 100 $\mu g\,ml^{-1}$. Protein extraction was done with the mixture of phenol : chloroform : isoamyl alcohol (25 : 24 : 1) twice followed with chloroform. DNA was precipitated with 2 volumes of absolute alcohol and 0.5 volume of 7.5 M ammonium acetate at −70°C overnight and recovered by centrifuging at 10,000 × *g* for 20 min at 4°C. The DNA was reconstructed with DNAse and RNAse-free water (Sigma Chemical Co, U.S.A.) and the quantity and quality were determined spectrophotometrically. DNA (10 μg per lane) was loaded onto a 2% agarose gel and electrophoresised at 25 V for 10 h. Ethidium bromide-stained DNA was visualized using the UV transilluminator at 302 nm and photographed using a polaroid camera.

TUNEL assay

Terminal deoxynucleotidyl transferase-mediated dUTP nick end labeling (TUNEL) assay was done to identify the extent of DNA fragmentation as previously reported (Kabra *et al*., 2004). Four groups (sham-, vehicle-, FeTMPyP- and FeTPPS-treated) each containing three rats were used for the TUNEL assay. After 70 h of reperfusion, rat was anesthetized and 200 ml of ice-cold phosphate-buffered saline was transcardially perfused followed by 500 ml of 4% buffered paraformaldehyde in saline (pH 7.4) for *in situ* fixation of brain. Brain was isolated, dehydrated and embedded in wax. Serial sections of 3 μm thickness were cut using microtome (Leica, Germany) and spread over microscopic slides. The sections at the level of anterior commissure, temporal limb (AP −0.26 to −0.51 mm to bregma), were selected for TUNEL assay. The 3′ end of the fragmented DNA was labeled using the DNA fragmentation detection kit–TdT-FragEL (Oncogene Research Products) according to the instructions given by the manufacturer. Briefly, the brain sections were prepared for labeling reaction by re-hydration followed by nuclear stripping (with proteinase K). Then the specimens were equilibrated with the TdT equilibration buffer and incubated with labeling reaction mixture in a humidification chamber for a period of 90 min at 37°C. The sections were mounted and observed under fluorescent microscope (Leica, Germany) and images were acquired with the CCD camera (Leica DC300F). The number of apoptotic nuclei was counted in four different fields and mean was found by using the image analysis software 'Leica Qwin'.

Statistical evaluation

Statistical analysis was performed using statistical analysis software Sigma Stat 2.0. Unless otherwise stated, all the results were expressed as mean ± s.e.m. Infarct and edema volumes were analyzed using one-way analysis of variance (ANOVA) followed by Tukey *post hoc* test. Neurological deficit scores were represented as median ± 95% confidence interval. They were analyzed using Kruskal–Wallis one-way analysis of variance (ANOVA) on ranks followed by Dunnett's test. TUNEL assay and rhodamine123 data were analyzed using one-way ANOVA followed by Tukey *post hoc* test. Differences were considered to be significant if $P<0.05$.

Results

Physiological variables

All physiological variables remained within normal limits during middle cerebral artery occlusion procedure. Rectal temperature was maintained at 37.0 ± 0.5°C. Oxygen flow rate in the anesthetic gas mixture was always fine titrated to get a pO_2 value of 135–160 mmHg, pCO_2 value of 30–45 mmHg and pH value of 7.3–7.5. The treatment groups tested did not differ with respect to pre-, intra- or post-ischemic rectal temperature, blood pressure, pO_2 and pCO_2 and pH, hemoglobin and serum glucose level. FeTMPyP and FeTPPS treatment did not alter any physiological parameter. The serum hemoglobin levels were $>9.5\,g\,dl^{-1}$ for all the animals included in the surgery. Before the administration of PDCs, the mean hemoglobin levels were 11.9 ± 0.3 and 12.3 ± 0.5 $g\,dl^{-1}$ for FeTMPyP and FeTPPS (3 $mg\,kg^{-1}$ 0.5 h post MCAO) treatment groups, respectively. At 10 min after reperfusion, the values were found to be 10.9 ± 0.6 and 12.5 ± 0.7 $g\,dl^{-1}$ for FeTMPyP and FeTPPS treatment groups, respectively. Blood glucose levels were found to be 108.2 ± 16.4 (before) and 119.7 ± 20.0 $mg\,dl^{-1}$ (after) for FeTMPyP and 122.0 ± 18 (before) and 115.5 ± 5.3 $mg\,dl^{-1}$ (after) for FeTPPS treatment groups, respectively. FeTMPyP and FeTPPS (3 $mg\,kg^{-1}$, i.v) treatment did not alter the blood pressure and heart rate.

Effect of FeTMPyP and FeTPPS on cerebral infarction

In all, 2 h of MCAO and 70 h of reperfusion resulted in a prominent infarction in the ipsilateral hemisphere (Table 1). Treatment with FeTMPyP produced statistically significant reduction in infarction at 2 and 6 h post MCAO as evident from TTC-stained sections (Figure 3a). FeTMPyP (0.3 and 1 $mg\,kg^{-1}$) treatment 2 h post MCAO significantly ($P<0.05$) reduced infarction by 49 and 66%, respectively. When FeTMPyP was administered at 1 $mg\,kg^{-1}$ 6 h post MCAO, it produced mild statistically insignificant reduction (32%) in infarct volume. Treatment with higher dose (3 $mg\,kg^{-1}$) 6 h post MCAO significantly reduced infarct volume (38%). FeTMPyP (1 and 3 $mg\,kg^{-1}$) treatment produced 30 and 38% (9 h post MCAO) and 9 and 15% (12 h post MCAO) reduction in infarct volume. Although treatment at latter time points reduced the infarct volume, statistical significance was not observed. FeTPPS treatment at 0.3 and 1 $mg\,kg^{-1}$, 2 h post MCAO produced significant ($P<0.05$) reduction (43 and 62%) in infarct volume, respectively (Figure 3b). FeTPPS (1 and 3 $mg\,kg^{-1}$) when administered 6 h post MCAO, produced statistically significant reduction (28 and 34%, respectively) in infarct volume. FeTPPS (1 and 3 $mg\,kg^{-1}$) treatment also produced 23 and 25% (9 h post MCAO groups) and 20 and 16% (12 h post MCAO groups) reduction in infarct volume. Statistical significance was, however, not observed in 9 and 12 h post MCAO FeTPPS treatment groups.

Effect of FeTMPyP and FeTPPS on cerebral edema

In all, 2 h of MCAO and 70 h of reperfusion resulted in a prominent increase in cerebral edema in the ipsilateral hemisphere as compared to contralateral hemisphere (Table 1). Treatment with FeTMPyP (0.3 and 1 $mg\,kg^{-1}$) 2 h post MCAO

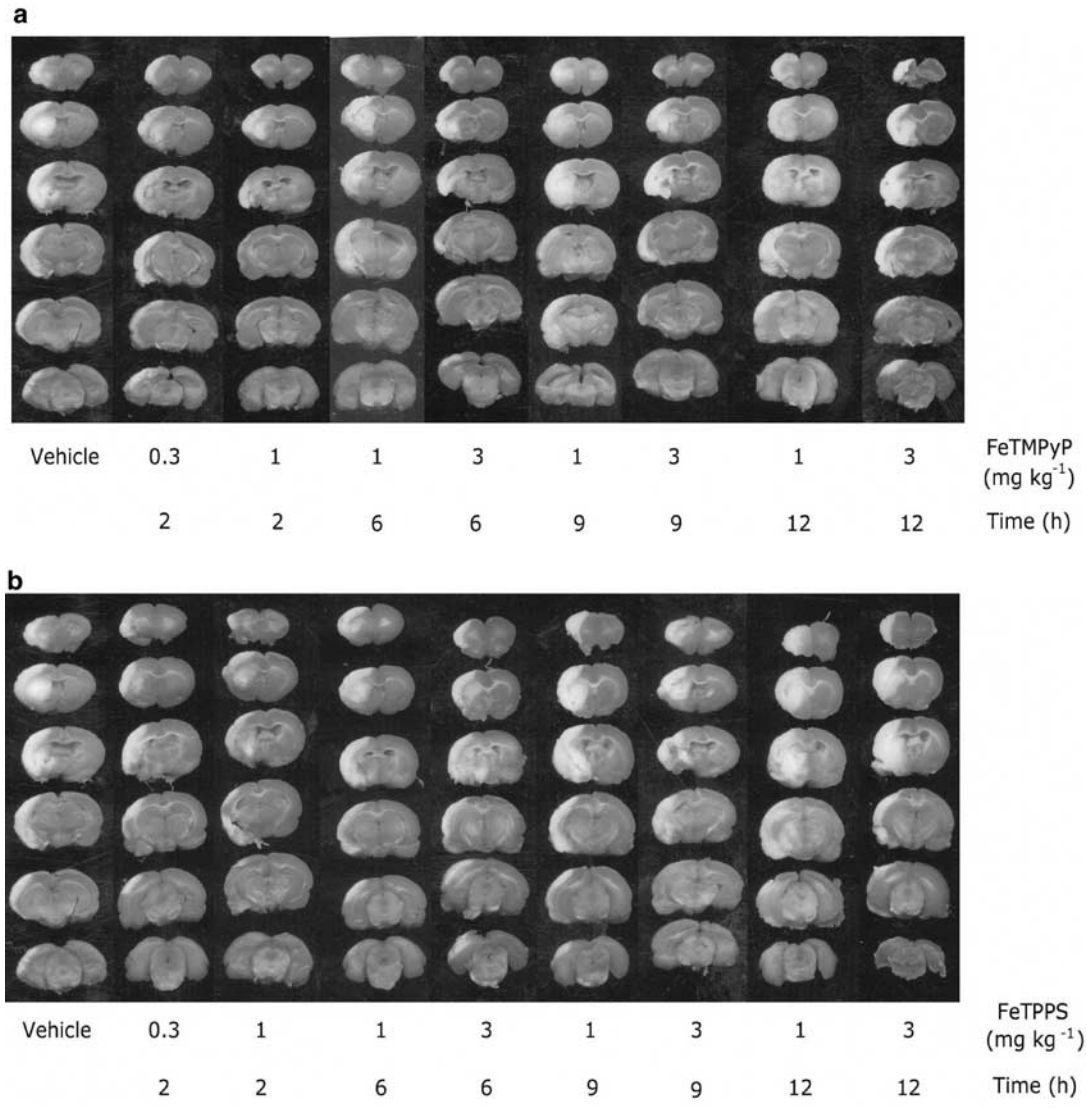

Figure 3 Representative coronal brain sections (2-mm thick) from FeTMPyP (a) (0.3 and 1 or 1 and 3 mg kg^{-1}) and FeTPPS (b) (0.3 and 1 or 1 and 3 mg kg^{-1})-treated rats stained with 2% triphenyl tetrazolium chloride (TTC) after 2 h of MCAO and 70 h of reperfusion showing infarction. FeTMPyP was administered at 2, 6, 9, 12 h post MCAO. Dark colored regions in the TTC-stained sections indicate nonischemic and pale colored regions indicate ischemic portion of brain.

produced 52 and 61% reduction in edema volume and FeTMPyP (1 and 3 mg kg^{-1}) treatment 6 h post MCAO produced 33 and 45% reduction in edema volume. The inhibition was found to be statistically significant in FeTMPyP (1 mg kg^{-1}) 2 h post MCAO treatment group as compared to the vehicle-treated group. FeTMPyP (1 and 3 mg kg^{-1}) treatment 9 h post MCAO produced 24 and 32% reduction in edema volume and FeTMPyP (1 and 3 mg kg^{-1}) treatment 12 h post MCAO reduced the edema volume to 26 and 33%, respectively. FeTPPS treatment up to 6 h post MCAO showed a significant decrease in edema volume as compared to vehicle-treated group. FeTPPS (0.3 and 1 mg kg^{-1}) treatment 2 h post MCAO produced 52 and 70% reduction in edema volume, whereas FeTPPS (1 and 3 mg kg^{-1}) treatment 6 h post MCAO produced 43 and 51% reduction in edema volume ($P<0.05$). FeTPPS (1 and 3 mg kg^{-1}) treatment 9 h post MCAO, inhibited edema to 31 and 41% and 12 h post MCAO treatment inhibited edema volume to 18 and 37%, respectively.

Effect of FeTMPyP and FeTPPS on neurological deficits

Vehicle-treated rats showed prominent neurological deficits (Table 1). FeTMPyP (1 mg kg^{-1}) treatment, 2 h post MCAO produced significant improvement in neurological score as compared to vehicle-treated control (Table 1). FeTPPS (3 mg kg^{-1}) treatment 6 h post MCAO showed a significant improvement in neurological function as compared to the vehicle-treated group. Though other groups did show a trend in the neurological improvement, statistical significance was not observed. Since FeTMPyP and FeTPPS treatment produced significant reduction in infarction, edema and neurological score at 3 mg kg^{-1} biochemical studies were performed at this dose only.

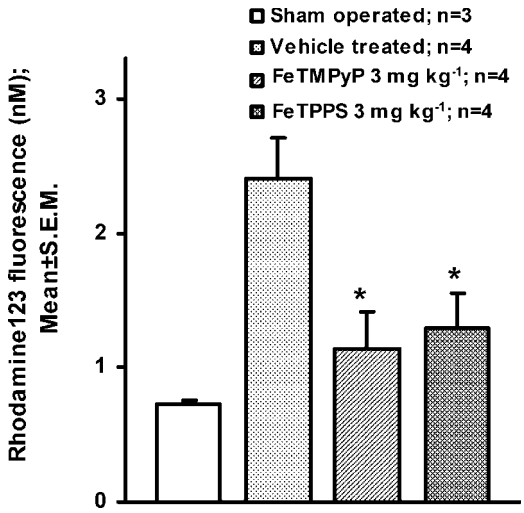

Figure 4 Dihydrorhodamine123 was injected to rats 1 h post MCAO and rhodamine123 fluorescence estimated in plasma 1 h post reperfusion in vehicle and FeTMPyP and FeTPPS (3 mg kg^{-1})-treated rat. Vehicle or FeTMPyP/FeTPPS (3 mg kg^{-1}) treatment was done 30 min post MCAO. The extent of rhodamine123 fluorescence reflects the extent of peroxynitrite formed during IR insult. FeTMPyP and FeTPPS treatment (3 mg kg^{-1}, i.v.) reduced the rhodamine123 fluorescence by decomposing peroxynitrite in a significant manner ($P<0.05$, F(2,9) = 6.59, ANOVA followed by Tukey Test).

Effect of FeTMPyP and FeTPPS on peroxynitrite concentration

Dihydrorhodamine123 is converted into rhodamine123 in a peroxynitrite-dependent manner. Peroxynitrite concentration estimated in plasma using dihydrorhodamine123 showed about 3.3-fold increase in rhodamine123 fluorescence in vehicle-treated MCAO rat as compared to sham-operated rat. FeTMPyP and FeTPPS (3 mg kg^{-1}, i.v) treatment reduced the ischemia-induced increase in the rhodamine123 fluorescence. The decrease in the rhodamine123 fluorescence was found to be statistically significant ($P<0.05$) (Figure 4). Tyrosine nitration, an index of nitrosative stress (presumably because of increased peroxynitrite), was estimated using immunofluorescence method in brain sections 2 h after MCAO and 4 h after reperfusion. With an anti-nitrotyrosine antibody and avidin FITC system, the immunoreactivity of nitrotyrosine residues was clearly observed in cytosol of neurons in the ipsilateral striatum and cortex (Figure 5b). On FeTMPyP and FeTPPS (3 mg kg^{-1}) treatment, the immunoreactivity decreased considerably in the ipsilateral striatum and cortex (Figure 5c and d).

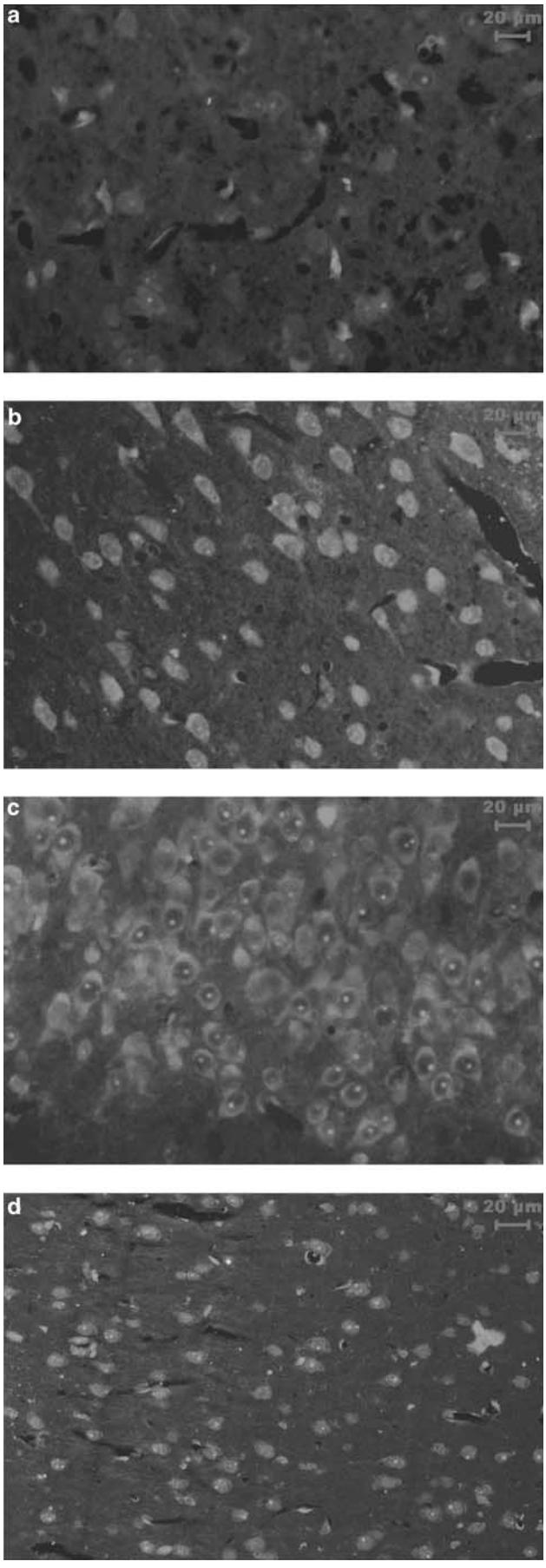

Figure 5 Immunofluorescence photomicrographs show nitrated tyrosine residues of cytosolic proteins. (a) Sham-operated rat brain section, (b) Vehicle-treated rat brain section ($n=3$). (c) FeTMPyP (3 mg kg^{-1}, i.v.)-treated animal ($n=3$). (d) FeTPPS (3 mg kg^{-1}, i.v.)-treated rat brain sections ($n=3$). Vehicle or FeTMPyP/FeTPPS (3 mg kg^{-1}) treatment was done 30 min post MCAO. All the FITC fluorescent images were acquired using the CCD camera (DC300F–Leica) with a constant exposure time of 0.805 s. FeTMPyP and FeTPPS treatment reduced the nitrotyrosine immunoreactivity.

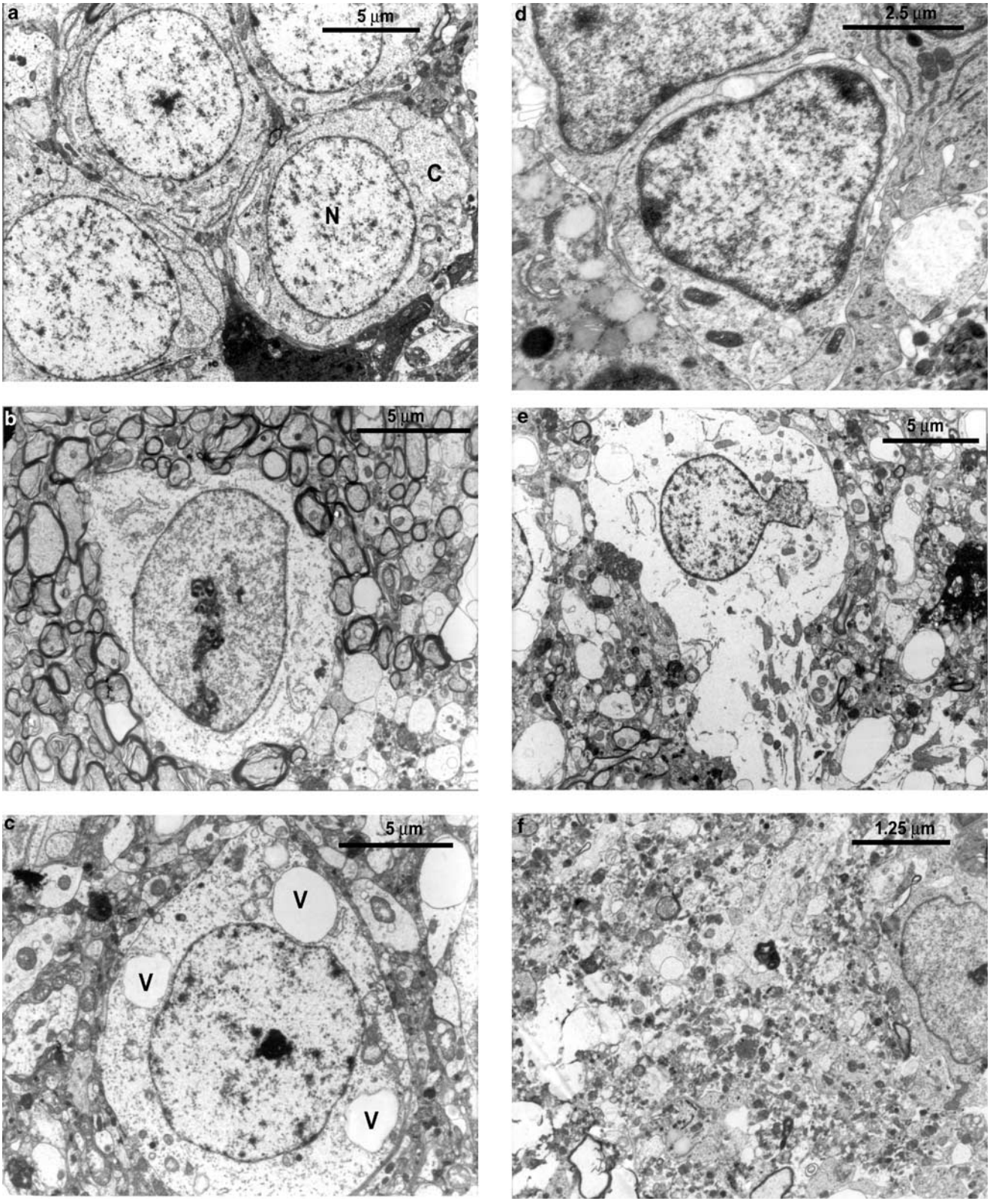

Figure 6 Electron photomicrographs of sham-operated and MCAO rat brain after 2 h of ischemia and 70 h MCAO. (a) Normal brain cells from sham-operated animal. N indicates nucleus and C indicates cytoplasm of the cell (b) Apoptotic cell in its early stage of apoptosis from the penumbral area of MCAO rat brain. The chromatin gets compacted and condensed on the inner surface of the nuclear membrane. (c) Vacuoles formed in the cytoplasm. V indicates vacuole. (d) At an advanced stage, more chromatin condensation occurs. This stage is followed by the formation of membrane-packed apoptotic bodies which are phagocytosed by the nearby glial cells. (e) Early necrotic cell: the cell membrane is ruptured and the cellular contents coming out of the cell. (f) Completely necrotic cell observed at the ischemic zone after 2 h of ischemia and 70 h MCAO.

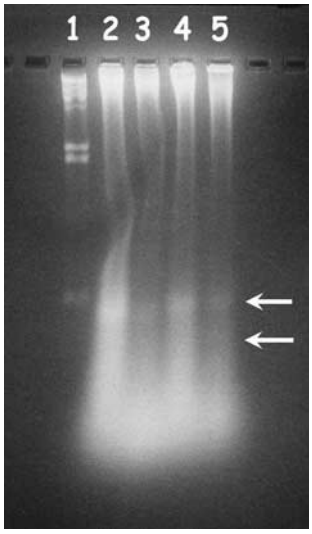

Figure 7 DNA ladder pattern observed in vehicle-treated and FeTMPyP-treated MCAO rats. Lane (1) Hind III digest (2) vehicle-treated ipsilateral penumbral cortex (3) FeTMPyP-treated ipsilateral penumbral cortex (4) vehicle-treated, ipsilateral ischemic cortex (5) FeTMPyP-treated ipsilateral ischemic cortex. The arrows indicate the fragmented DNA.

Effect of FeTMPyP and FeTPPS on apoptosis

Delayed neuronal loss after cerebral ischemia has been reported to be apoptotic in nature. To characterize the same, brain sections from sham-operated and ischemic animals (penumbral and ischemic core regions) were analyzed using electron microscope. Brain sections from the sham-operated rat showed normal features of cell, whereas the sections from ischemic animals showed characteristic features of apoptotic and necrotic cell death (Figure 6). To further analyze the apoptotic neuronal death and to see whether PDC treatment reduces the apoptosis, DNA ladder pattern was studied. FeTMPyP ($3\,mg\,kg^{-1}$) treatment resulted in a prominent decrease in the DNA ladder formation (Figure 7). In TUNEL assay, brain sections from sham-operated group showed only slight background staining with no TUNEL-positive cells (Figure 8a I). Brain sections from vehicle-treated ischemic rat showed an increase in TUNEL-positive cells (Figure 8a II). The positively stained apoptotic nuclei were observed in the penumbral areas of ipsilateral hemisphere. Increase in TUNEL-positive cells was reduced by FeTMPyP and FeTPPS ($3\,mg\,kg^{-1}$) treatment (Figure 8a III and IV). Reduction in TUNEL-positive cells was found to be 48 and 40% in FeTMPyP and FeTPPS ($3\,mg\,kg^{-1}$)-treated groups, respectively (Figure 8b).

Discussion

In the present study, PDCs, FeTMPyP and FeTPPS produced significant neuroprotection in focal cerebral ischemia, as evident from significant reduction in cerebral infarction, edema and neurological deficits. The neuroprotection was found to be maximal at 2 h post MCAO ($1\,mg\,kg^{-1}$) treatment groups. FeTMPyP ($3\,mg\,kg^{-1}$) and FeTPPS ($3\,mg\,kg^{-1}$) treatment even up to 6 h post MCAO produced significant reduction (42 and 30%, respectively) in infarct volume. Delayed FeTPPS ($3\,mg\,kg^{-1}$) treatment even up to 6 h post MCAO reduced edema volume and improved neurological deficits. Although FeTPPS and FeTMPyP (1 and $3\,mg\,kg^{-1}$) reduced the infarction, edema volume and neurological deficits, at latter time points (9 and 12 h post MCAO) the reduction was found to be statistically insignificant. Several neuroprotective agents have been found to produce considerable neuroprotection if treatment is scheduled before or during IR insult, but they often fail at clinical trials. Hence, the therapeutic time window becomes an important parameter to study and evaluate the neuroprotective efficacy (Roundtable, 1999) of FeTMPyP and FeTPPS. In *in vitro* studies, FeTMPyP showed cytoprotection in endogenously generated peroxynitrite in endotoxin-stimulated RAW 264.7 cells as well as in culture of hippocampal neurons and glial cells that had been exposed to cytokines (Misko *et al*., 1998). They were also shown to ameliorate carrageenan-induced paw edema (Salvemini *et al*., 1998). In *in vivo* studies, FeTMPyP showed protection against methamphetamine-induced neurotoxicity and in the splanchic artery occlusion and reperfusion model in rat (Imam *et al*., 1999; Cuzzocrea *et al*., 2000b). FeTMPyP also reported to modulate p38 and NF-κB in thymocytes (Kang *et al*., 2003). FP-15, a new peroxynitrite decomposition catalyst, has been reported to prevent myocardial infarction in pigs (Bianchi *et al*., 2002), lung ischemia (Naidu *et al*., 2003) and arthritis and colitis (Mabley *et al*., 2002) in mice.

During ischemia, brain NO level rises from $<10\,nM$ to $1\,\mu M$ within 3–24 min (Malinski *et al*., 1993). The initial rise in NO is a result of activation of constitutive NOS (probably as a result of excitotoxicity) in a $[Ca^{2+}]_i$-dependent manner. Cytokines like TNFα, interleukin 1β and interferon γ were reported to increase after IR insult (Schroeter *et al*., 2003). Cytokine upregulation becomes one of the key stimuli for the iNOS activation (Hurtado *et al*., 2001; Mizushima *et al*., 2002). iNOS-mediated NO increase occurs as early as 4 h after MCAO (Nagafuji *et al*., 1994). In transient forebrain ischemia model, mRNA for iNOS and immunoreactivity of iNOS peaks 12 h after IR insult (Iadecola *et al*., 1996). iNOS upregulation as a result of various cytokines results in continuous production of NO. During IR insult, large quantities of superoxide are also produced. During the ischemic phase, xanthine dehydrogenase, an enzyme which is involved in purine metabolism, is irreversibly converted to xanthine oxidase by sulfhydryl cleavage. Supply of molecular oxygen during the reperfusion phase (which serves as a substrate for xanthine oxidase for nucleotide metabolism) results in the production of a heavy burst of superoxide as byproduct. Xanthine oxidase-derived superoxide formation accounts for the major contribution of total superoxide produced during IR injury (McCord, 1985). Chemotactic recruitment of leukocyte occurs within hours after IR insult in the ischemic brain. Adhesion of activated leukocytes to the internal lumen of blood capillaries not only produces a secondary occlusion, rather high concentrations of superoxide are continuously released from the activated leukocytes. Metallophorphyrin SOD mimetics (MnTE-2-PyP(5+), AEOL 10113 and AEOL 10150) treatment (upto 6 h post MCAO) reduced ischemic damage in mice and rat (Mackensen *et al*., 2001; Sheng *et al*., 2002), indicating that the superoxide is produced continuously till several hours after the IR insult and contributes to the neuronal loss. The formation of superoxide and NO can result

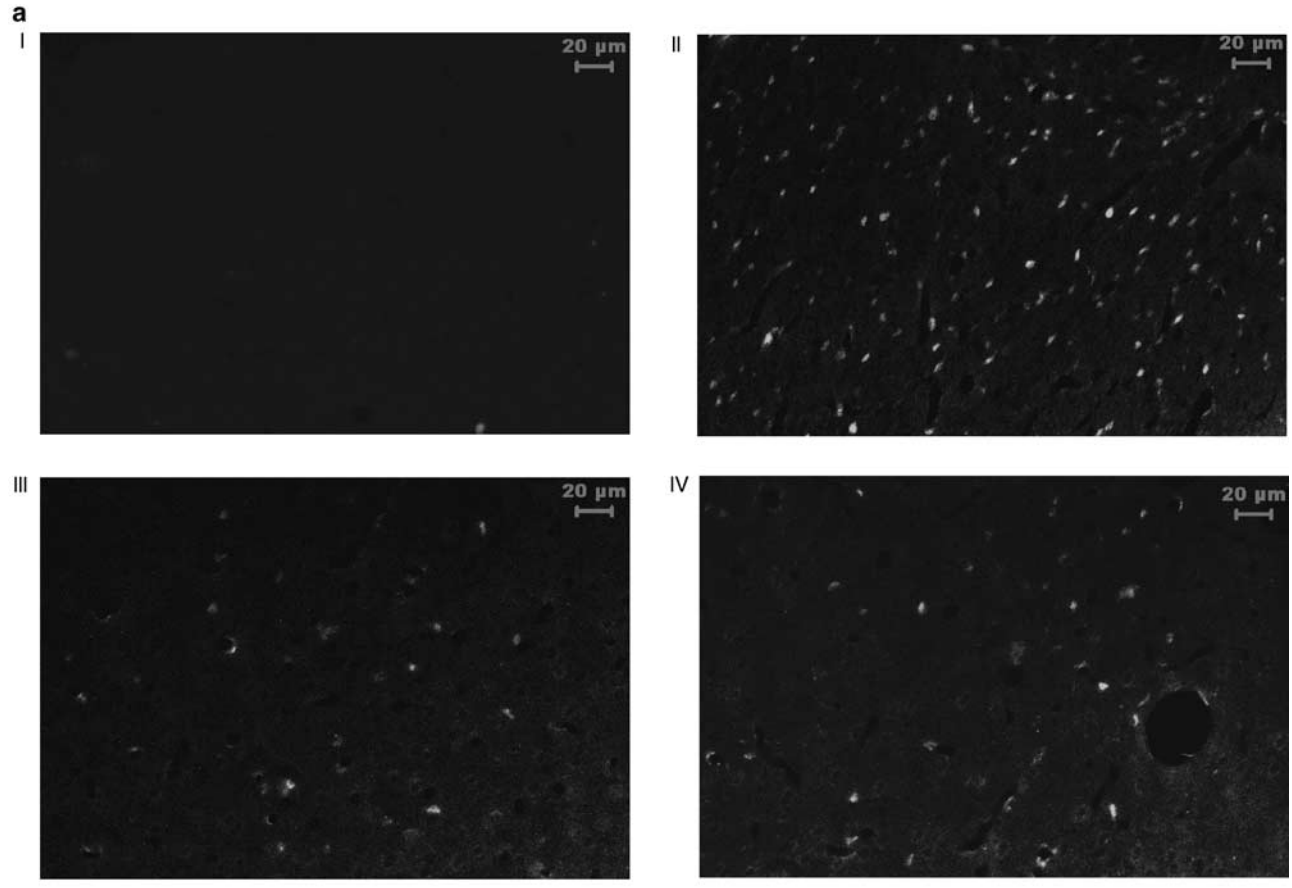

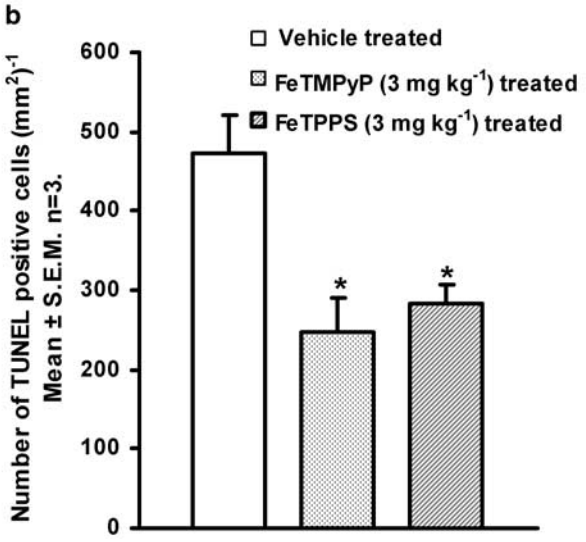

Figure 8 (a) Representative photomicrographs of saline (vehicle), FeTMPyP or FeTPPS ($3\,mg\,kg^{-1}$, i.v.)-treated ($n=3$ in each group) MCAO rat brain sections at the level of anterior commissure, temporal limb (AP = −0.26 to −0.51 mm to bregma) labeled with DNA nick end-labeling (TUNEL) method. (I) Sham-operated rat brain sections after TUNEL. (II) Vehicle-treated rat brain sections labeled according to TUNEL method. The TUNEL-positive cells were observed in the ischemic and penumbral area of cerebral cortex and striatum. (III) FeTMPyP ($3\,mg\,kg^{-1}$ i.v)-treated rat brain sections labeled according to TUNEL method. (IV) FeTPPS ($3\,mg\,kg^{-1}$ i.v)-treated rat brain sections labeled according to TUNEL method. (b) TUNEL-positive cells were counted in each field (dimensions 0.42×0.35 mm) using Leica Qwin image analysis software and the cell count obtained from the same group of rats were averaged and translated to the number of positive cells per mm^3. FeTMPyP and FeTPPS ($3\,mg\,kg^{-1}$, i.v.) treatment significantly reduced the number of TUNEL-positive cells in the penumbral area ($P<0.05$, $F(2,9)=9.25$, ANOVA followed by Tukey test). Statistical significance was evaluated using one-way analysis of variance. *$P<0.05$ as compared to the vehicle-treated group.

in the formation of peroxynitrite in the affected region. NO_2^- and NO_3^- (catabolic products of peroxynitrite) concentrations reported to peak 30–48 h after the head injury (Clark *et al*., 1996) indicate that peroxynitrite formation is a late event after injury. Similar observations have been made in the myocardial ischemia model (Akiyama *et al*., 1997). We speculate that the main reason for the neuroprotective activity of PDCs in the present study is at least in part as a result of decomposition of endogenously generated peroxynitrite and superoxide.

PDCs may have higher efficacy as compared to selective metalloporphyrin SOD mimetics because dismutation of superoxide results in accumulation of hydrogen peroxide, which can produce toxic $HO^{\bullet}$ (i.e. SOD acts as pro-oxidant) (Yim *et al*., 1990) unless catalase mimetics are co-administered or catalase is upregulated in the system. Experiments conducted by Gobbel and co-workers in cerebral endothelial cells showed toxicities of 26 and 11% (as evident from lactate dehydrogenase release) on treatment with 1 mM of sodium nitroprusside and 0.2 mM paraquat, respectively (sodium nitroprusside and paraquat release nitric oxide and superoxide, respectively). However, when they were combined together, the toxicity increased to 78.8% (Gobbel *et al*., 1997) as a result of formation of peroxynitrite. This is a very clear example to demonstrate the toxic effects mediated by nitric oxide, superoxide and peroxynitrite on relative terms. Misko and co-workers (1998) showed that, Mn analog (SOD mimetics) of the porphyrine is less efficacious than the corresponding Fe analog (PDCs) in mediating the neuroprotection in RAW cell lines, which are treated with lipopolysaccharide (Misko *et al*., 1998). In addition to peroxynitrite-decomposing effect, FeTMPyP and FeTPPS do demonstrate moderate superoxide dismutase effect (Lee *et al*., 1998). In fact, the peroxynitrite-decomposing effect increases considerably if superoxide and peroxynitrite are present in the same milieu as a result of the formation of catalytic cycle (Lee *et al*., 1998). Based on these, we expected that FeTMPyP and FeTPPS might be better candidates to treat IR injury, where the increase of superoxide and NO happens simultaneously, resulting in continuous formation of peroxynitrite.

To observe whether PDC treatment indeed reduces the peroxynitrite in *in vivo* condition, we estimated rhodamine123 fluorescence in rat serum. FeTMPyP ($3\,mg\,kg^{-1}$) and FeTPPS ($3\,mg\,kg^{-1}$) treatment produced almost complete reversal of peroxynitrite-mediated conversion of dihydrorhodamine123 to rhodamine123, indicating faster clearance of peroxynitrite by FeTMPyP and FeTPPS. The increase in nitrosative stress presumably mediated by peroxynitrite reaction was monitored by measuring the extent of tyrosine nitration in cytosolic proteins using immunofluorescence technique in brain sections. In this study, as well as in our earlier study, we observed a significant increase in immunoreactivity of nitrotyrosine after IR insult (Thiyagarajan & Sharma, 2004). If peroxynitrite is decomposed by FeTMPyP and FeTPPS treatment, this would have resulted in lesser nitrotyrosine formation and hence lower immunoreactivity. The same has been observed in the immunofluorescence experiments, indicating that the neuroprotective effect of FeTMPyP and FeTPPS is at least in part as a result of peroxynitrite decomposition.

The ischemic core which forms immediately after the IR insult invariably expands outwards, resulting in a higher infarct volume measured after 72 h of ischemia as compared to that of early time points. It is well documented that the delayed neuronal loss in the penumbral area after the IR insult is apoptotic in nature (Schmidt-Kastner *et al*., 1997; Tagaya *et al*., 1997). To confirm the occurrence of apoptosis-mediated cell death, we examined the sham-operated and MCAO-induced ischemic brain specimens from infarct and penumbral zone using electron microscope (Figure 6). As peroxynitrite can induce apoptotic cell death (Estevez *et al*., 1995; Virag *et al*., 1998) and as peroxynitrite concentration rises during IR insult, we wanted to find whether IR insult-mediated apoptotic neuronal loss is mediated by peroxynitrite. If so, could peroxynitrite-mediated apoptotic neuronal loss be inhibited by PDCs? To answer this question, we examined the DNA ladder pattern and estimated the extent of apoptosis using TUNEL method. As delayed FeTMPyP ($3\,mg\,kg^{-1}$) treatment (6 h post MCAO) produced significant reduction in infarct volume, we thought that FeTMPyP-mediated neuroprotection may be at least in part as a result of reduction in delayed neuronal death. In DNA ladder experiments, FeTMPyP ($3\,mg\,kg^{-1}$) treatment showed a prominent reduction in DNA ladder pattern (Figure 7). FeTMPyP ($3\,mg\,kg^{-1}$) treatment also reduced the TUNEL-positive cells observed in the ipsilateral penumbral zone. These experiments confirm that FeTMPyP ($3\,mg\,kg^{-1}$) treatment-mediated neuroprotection is at least in part as a result of reduction of apoptosis. Many antioxidants including ebselen and EPC-K1 have been reported to reduce the extent of apoptotic cell death (Namura *et al*., 2001; Zhang *et al*., 2001).

This study demonstrated the neuroprotective effects of peroxynitrite decomposition catalysts (FeTMPyP and FeTPPS) in focal cerebral ischemia in rats. These agents were effective even if administered 6 h post MCAO. Neuroprotective effect is at least in part due to the reduction of nitrotyrosine formation and apoptosis. This study has significant implications since protection with PDCs has also been observed in other neurotoxicity models.

This study was supported by grants from NIPER (NP035) and DST Young Scientists Fast Track Scheme (SR/FTP/LS-A-36/2001) to S.S. Sharma. We gratefully acknowledge Professor K.P.R. Kartha, Department of Medicinal Chemistry, NIPER, for his help in spelling and grammar correction of this article. We acknowledge the Electron Microscopy Section of All India Institute of Medical Sciences, New Delhi, India, for their help in conducting electron microscopy for this study.

References

AKIYAMA, K., SUZUKI, H., GRANT, P. & BING, R.J. (1997). Oxidation products of nitric oxide, NO_2 and NO_3, in plasma after experimental myocardial infarction. *J. Mol. Cell. Cardiol.,* **29,** 1–9.

BECKMAN, J.S., CHEN, J., CROW, J.P. & YE, Y.Z. (1994). Reactions of nitric oxide, superoxide and peroxynitrite with superoxide dismutase in neurodegeneration. *Prog. Brain Res.,* **103,** 371–380.

BECKMAN, J.S., ISCHIROPOULOS, H., ZHU, L., VAN DER WOERD, M., SMITH, C., CHEN, J., HARRISON, J., MARTIN, J.C. & TSAI, M. (1992). Kinetics of superoxide dismutase- and iron-catalyzed nitration of phenolics by peroxynitrite. *Arch. Biochem. Biophys.,* **298,** 438–445.

BIANCHI, C., WAKIYAMA, H., FARO, R., KHAN, T., MCCULLY, J.D., LEVITSKY, S., SZABO, C. & SELLKE, F.W. (2002). A novel peroxynitrite decomposer catalyst (FP-15) reduces myocardial infarct size in an *in vivo* peroxynitrite decomposer and acute ischemia–reperfusion in pigs. *Ann. Thorac. Surg.,* **74,** 1201–1207.

CASTRO, L., RODRIGUEZ, M. & RADI, R. (1994). Aconitase is readily inactivated by peroxynitrite, but not by its precursor, nitric oxide. *J. Biol. Chem.,* **269,** 29409–29415.

CLARK, R.S., KOCHANEK, P.M., OBRIST, W.D., WONG, H.R., BILLIAR, T.R., WISNIEWSKI, S.R. & MARION, D.W. (1996). Cerebrospinal fluid and plasma nitrite and nitrate concentrations after head injury in humans. *Crit. Care. Med.,* **24,** 1243–1251.

CLEMENS, J.A., HO, P.P. & PANETTA, J.A. (1991). LY178002 reduces rat brain damage after transient global forebrain ischemia. *Stroke,* **22,** 1048–1052.

CUZZOCREA, S., MCDONALD, M.C., MAZZON, E., SIRIWARDENA, D., COSTANTINO, G., FULIA, F., CUCINOTTA, G., GITTO, E., CORDARO, S., BARBERI, I., DE SARRO, A., CAPUTI, A.P. & THIEMERMANN, C. (2000a). Effects of tempol, a membrane-permeable radical scavenger, in a gerbil model of brain injury. *Brain Res.,* **875,** 96–106.

CUZZOCREA, S., MISKO, T.P., COSTANTINO, G., MAZZON, E., MICALI, A., CAPUTI, A.P., MACARTHUR, H. & SALVEMINI, D. (2000b). Beneficial effects of peroxynitrite decomposition catalyst in a rat model of splanchnic artery occlusion and reperfusion. *FASEB J.,* **14,** 1061–1072.

CUZZOCREA, S., RILEY, D.P., CAPUTI, A.P. & SALVEMINI, D. (2001). Antioxidant therapy: a new pharmacological approach in shock, inflammation, and ischemia/reperfusion injury. *Pharmacol. Rev.,* **53,** 135–159.

DENICOLA, A., FREEMAN, B.A., TRUJILLO, M. & RADI, R. (1996). Peroxynitrite reaction with carbon dioxide/bicarbonate: kinetics and influence on peroxynitrite-mediated oxidations. *Arch. Biochem. Biophys.,* **333,** 49–58.

ESTEVEZ, A.G., RADI, R., BARBEITO, L., SHIN, J.T., THOMPSON, J.A. & BECKMAN, J.S. (1995). Peroxynitrite-induced cytotoxicity in PC12 cells: evidence for an apoptotic mechanism differentially modulated by neurotrophic factors. *J. Neurochem.,* **65,** 1543–1550.

FUSON, K.S., MARK, R.J., PANETTA, J.A. & MAY, P.C. (1999). Characterization of LY231617 protection against hydrogen peroxide toxicity. *J. Neurochem.,* **72,** 1154–1160.

GOBBEL, G.T., CHAN, T.Y. & CHAN, P.H. (1997). Nitric oxide- and superoxide-mediated toxicity in cerebral endothelial cells. *J. Pharmacol. Exp. Ther.,* **282,** 1600–1607.

GUPTA, S., KAUL, C. & SHARMA, S. (2004). Neuroprotective effect of combination of poly (ADP-ribose) polymerase inhibitor and antioxidant in middle cerebral artery occlusion induced focal ischemia in rats. *Neurol. Res.,* **26,** 103–107.

HURTADO, O., CARDENAS, A., LIZASOAIN, I., BOSCA, L., LEZA, J.C., LORENZO, P. & MORO, M.A. (2001). Up-regulation of TNF-α convertase (TACE/ADAM17) after oxygen-glucose deprivation in rat forebrain slices. *Neuropharmacology,* **40,** 1094–1102.

IADECOLA, C., ZHANG, F., CASEY, R., CLARK, H.B. & ROSS, M.E. (1996). Inducible nitric oxide synthase gene expression in vascular cells after transient focal cerebral ischemia. *Stroke,* **27,** 1373–1380.

IMAIZUMI, S., KAYAMA, T. & SUZUKI, J. (1984). Chemiluminescence in hypoxic brain – the first report. Correlation between energy metabolism and free radical reaction. *Stroke,* **15,** 1061–1065.

IMAM, S.Z., CROW, J.P., NEWPORT, G.D., ISLAM, F., SLIKKER JR, W. & ALI, S.F. (1999). Methamphetamine generates peroxynitrite and produces dopaminergic neurotoxicity in mice: protective effects of peroxynitrite decomposition catalyst. *Brain Res.,* **837,** 15–21.

IMAM, S.Z., El-YAZAL, J., NEWPORT, G.D., ITZHAK, Y., CADET, J.L., SLIKKER, W., JR & ALI, S.F. (2001). Methamphetamine-induced dopaminergic neurotoxicity: role of peroxynitrite and neuroprotective role of antioxidants and peroxynitrite decomposition catalysts. *Ann. N. Y. Acad. Sci.,* **939,** 366–380.

JONNALA, R.R. & BUCCAFUSCO, J.J. (2001). Inhibition of nerve growth factor signaling by peroxynitrite. *J. Neurosci. Res.,* **63,** 27–34.

KABRA, D., THIYAGARAJAN, M., KAUL, C.L. & SHARMA, S.S. (2004). Neuroprotective effect of 4-amino 1, 8-napthalimide, a poly (ADP ribose) polymerase inhibitor in middle cerebral artery occlusion induced focal cerebral ischemia in rat. *Brain Res. Bull.,* **62,** 425–433.

KANG, J.L., LEE, H.S., JUNG, H.J. & KIM, H.J. (2003). Iron tetrakis (*N*-methyl-4′-pyridyl) porphyrinato inhibits proliferative activity of thymocytes by blocking activation of p38 mitogen-activated protein kinase, nuclear factor-kappaB, and interleukin-2 secretion. *Toxicol. Appl. Pharmacol.,* **191,** 147–155.

KING, P.A., ANDERSON, V.E., EDWARDS, J.O., GUSTAFSON, G., PLUMB, R.C. & SUGGS, J.W. (1992). A stable solid that generates hydroxyl radical upon dissolution in aqueous solutions: reaction with proteins and nucleic acid. *J. Am. Chem. Soc.,* **114,** 5430–5432.

KUMURA, E., YOSHIMINE, T., IWATSUKI, K.I., YAMANAKA, K., TANAKA, S., HAYAKAWA, T., SHIGA, T. & KOSAKA, H. (1996). Generation of nitric oxide and superoxide during reperfusion after focal cerebral ischemia in rats. *Am. J. Physiol.,* **270,** C748–C752.

LEE, J., HUNT, J. & GROVES, J.T. (1998). Mechanisms of iron porphyrin reactions with peroxynitrite. *Am. J. Chem. Soc.,* **120,** 7493–7501.

LONGA, E.Z., WEINSTEIN, P.R., CARLSON, S. & CUMMINS, R. (1989). Reversible middle cerebral artery occlusion without craniectomy in rats. *Stroke,* **20,** 84–91.

MABLEY, J.G., LIAUDET, L., PACHER, P., SOUTHAN, G.J., SALZMAN, A.L. & SZABO, C. (2002). Part II: beneficial effects of the peroxynitrite decomposition catalyst FP15 in murine models of arthritis and colitis. *Mol. Med.,* **8,** 581–590.

MACKENSEN, G.B., PATEL, M., SHENG, H., CALVI, C.L., BATINIC-HABERLE, I., DAY, B.J., LIANG, L.P., FRIDOVICH, I., CRAPO, J.D., PEARLSTEIN, R.D. & WARNER, D.S. (2001). Neuroprotection from delayed postischemic administration of a metalloporphyrin catalytic antioxidant. *J. Neurosci.,* **21,** 4582–4592.

MALINSKI, T., BAILEY, F., ZHANG, Z.G. & CHOPP, M. (1993). Nitric oxide measured by a porphyrinic microsensor in rat brain after transient middle cerebral artery occlusion. *J. Cereb. Blood Flow Metab.,* **13,** 355–358.

MARLA, S.S., LEE, J. & GROVES, J.T. (1997). Peroxynitrite rapidly permeates phospholipid membranes. *Proc. Natl. Acad. Sci. U.S.A.,* **94,** 14243–14248.

MCCORD, J.M. (1985). Oxygen-derived free radicals in postischemic tissue injury. *N. Engl. J. Med.,* **312,** 159–163.

MISKO, T.P., HIGHKIN, M.K., VEENHUIZEN, A.W., MANNING, P.T., STERN, M.K., CURRIE, M.G. & SALVEMINI, D. (1998). Characterization of the cytoprotective action of peroxynitrite decomposition catalysts. *J. Biol. Chem.,* **273,** 15646–15653.

MIZUSHIMA, H., ZHOU, C.J., DOHI, K., HORAI, R., ASANO, M., IWAKURA, Y., HIRABAYASHI, T., ARATA, S., NAKAJO, S., TAKAKI, A., OHTAKI, H. & SHIODA, S. (2002). Reduced postischemic apoptosis in the hippocampus of mice deficient in interleukin-1. *J. Comp. Neurol.,* **448,** 203–216.

MURAKAMI, K., KONDO, T., KAWASE, M., LI, Y., SATO, S., CHEN, S.F. & CHAN, P.H. (1998). Mitochondrial susceptibility to oxidative stress exacerbates cerebral infarction that follows permanent focal cerebral ischemia in mutant mice with manganese superoxide dismutase deficiency. *J. Neurosci.,* **18,** 205–213.

NAGAFUJI, T., SUGIYAMA, M. & MATSUI, T. (1994). Temporal profiles of Ca2+/calmodulin-dependent and -independent nitric oxide synthase activity in the rat brain microvessels following cerebral ischemia. *Acta. Neurochir. Suppl. (Wien),* **60,** 285–288.

NAIDU, B.V., FRAGA, C., SALZMAN, A.L., SZABO, C., VERRIER, E.D. & MULLIGAN, M.S. (2003). Critical role of reactive nitrogen species in lung ischemia–reperfusion injury. *J. Heart Lung Transplant.,* **22,** 784–793.

NAMURA, S., NAGATA, I., TAKAMI, S., MASAYASU, H. & KIKUCHI, H. (2001). Ebselen reduces cytochrome *c* release from mitochondria and subsequent DNA fragmentation after transient focal cerebral ischemia in mice. *Stroke,* **32,** 1906–1911.

PATEL, M. & DAY, B.J. (1999). Metalloporphyrin class of therapeutic catalytic antioxidants. *Trends Pharmacol. Sci.,* **20,** 359–364.

RADI, R., BECKMAN, J.S., BUSH, K.M. & FREEMAN, B.A. (1991). Peroxynitrite-induced membrane lipid peroxidation: the cytotoxic potential of superoxide and nitric oxide. *Arch. Biochem. Biophys.,* **288,** 481–487.

ROUNDTABLE, S.T.A.I. (1999). Recommendations for standards regarding preclinical neuroprotective and restorative drug development. *Stroke,* **30,** 2752–2758.

SALGO, M.G., SQUADRITO, G.L. & PRYOR, W.A. (1995). Peroxynitrite causes apoptosis in rat thymocytes. *Biochem. Biophys. Res. Commun.,* **215,** 1111–1118.

SALVEMINI, D., WANG, Z.Q., STERN, M.K., CURRIE, M.G. & MISKO, T.P. (1998). Peroxynitrite decomposition catalysts: therapeutics for peroxynitrite-mediated pathology. *Proc. Natl. Acad. Sci. U.S.A.,* **95,** 2659–2663.

SALVEMINI, D., WANG, Z.Q., ZWEIER, J.L., SAMOUILOV, A., MACARTHUR, H., MISKO, T.P., CURRIE, M.G., CUZZOCREA, S., SIKORSKI, J.A. & RILEY, D.P. (1999). A nonpeptidyl mimic of superoxide dismutase with therapeutic activity in rats. *Science,* **286,** 304–306.

SCHMIDT-KASTNER, R., FLISS, H. & HAKIM, A.M. (1997). Subtle neuronal death in striatum after short forebrain ischemia in rats detected by *in situ* end-labeling for DNA damage. *Stroke,* **28,** 163–169 (discussion 169-170).

SCHROETER, M., KURY, P. & JANDER, S. (2003). Inflammatory gene expression in focal cortical brain ischemia: differences between rats and mice. *Brain Res. Mol. Brain Res.,* **117,** 1–7.

SHENG, H., ENGHILD, J.J., BOWLER, R., PATEL, M., BATINIC-HABERLE, I., CALVI, C.L., DAY, B.J., PEARLSTEIN, R.D., CRAPO, J.D. & WARNER, D.S. (2002). Effects of metalloporphyrin catalytic antioxidants in experimental brain ischemia. *Free Radic. Biol. Med.,* **33,** 947–961.

SMITH, C.D., CARSON, M., VAN DER WOERD, M., CHEN, J., ISCHIROPOULOS, H. & BECKMAN, J.S. (1992). Crystal structure of peroxynitrite-modified bovine Cu,Zn superoxide dismutase. *Arch. Biochem. Biophys.,* **299,** 350–355.

SZABO, C., SALZMAN, A.L. & ISCHIROPOULOS, H. (1995). Peroxynitrite-mediated oxidation of dihydrorhodamine 123 occurs in early stages of endotoxic and hemorrhagic shock and ischemia–reperfusion injury. *FEBS Lett.,* **372,** 229–232.

TAGAYA, M., LIU, K.F., COPELAND, B., SEIFFERT, D., ENGLER, R., GARCIA, J.H. & DEL ZOPPO, G.J. (1997). DNA scission after focal brain ischemia. Temporal differences in two species. *Stroke,* **28,** 1245–1254.

THIYAGARAJAN, M. & SHARMA, S.S. (2004). Neuroprotective effect of curcumin in middle cerebral artery occlusion induced focal cerebral ischemia in rats. *Life Sci.,* **74,** 969–984.

VIRAG, L., SCOTT, G.S., CUZZOCREA, S., MARMER, D., SALZMAN, A.L. & SZABO, C. (1998). Peroxynitrite-induced thymocyte apoptosis: the role of caspases and poly (ADP-ribose) synthetase (PARS) activation. *Immunology,* **94,** 345–355.

YIM, M.B., CHOCK, P.B. & STADTMAN, E.R. (1990). Copper, zinc superoxide dismutase catalyzes hydroxyl radical production from hydrogen peroxide. *Proc. Natl. Acad. Sci. U.S.A.,* **87,** 5006–5010.

ZHANG, W.R., HAYASHI, T., SASAKI, C., SATO, K., NAGANO, I., MANABE, Y. & ABE, K. (2001). Attenuation of oxidative DNA damage with a novel antioxidant EPC-K1 in rat brain neuronal cells after transient middle cerebral artery occlusion. *Neurol. Res.,* **23,** 676–680.

(Received January 1, 2004
Revised February 26, 2004
Accepted March 25, 2004)